

MODELLING SHALLOW WATER SOUND TRANSMISSION BY USING A SIMPLE ANALYTICAL FORMULA BASED ON THE EFFECTIVE DEPTH APPROXIMATION

Zhi Yong Zhang

Defence Science & Technology Group
PO Box 1500 Edinburgh, SA 5111, Australia
Email: yong.zhang@dsto.defence.gov.au

Abstract

Understanding and modelling the transmission of underwater sound is critical for predicting the performance of acoustic sensing systems. Complicated mathematical models based on various approaches have been developed in past decades to predict sound transmission in the complex underwater environments. These complex models require detailed environmental inputs, longer execution time, and do not always show explicitly the effects of specific environment factors. For quick engineering assessments or sonar operations analysis, it would be advantageous to develop simple parameterised sound transmission formulas that capture the main features of underwater sound propagation using the fewest possible parameters. In this paper, we give a simple formula for incoherently averaged transmission loss in shallow water environments by taking into account the effects of energy spreading, absorption, and leakage out of boundaries. The formula is based on extension of earlier work by using the concept of effective depth to include the effect of normal mode penetration into the seafloor on modal attenuation. Comparison with measurement data at several shallow water sites worldwide shows that the formula are capable of producing the main features of shallow water sound propagation in environments with different types of seafloors. The formulas are useful for estimating sound transmission losses in generic yet representative underwater environments where detailed environmental knowledge is lacking or the fine details of underwater sound propagation is not required.

1. Introduction

Understanding the transmission of sound in the undersea environment is critical for predicting the performance of underwater acoustic sensing systems. Various complex mathematical models, based on various approaches (e.g., rays, modes, Gaussian beams, parabolic equations approximations, numerical integration, finite differences, finite elements, etc) have been developed to predict sound transmission, taking into account the effects of the underwater environment including refraction and attenuation in the media, and reflection and scattering from the boundaries (Etter, 2013; Jensen et al., 2013). These complex models require detailed environmental inputs, longer execution time, and do not show explicitly the effects of specific environmental factors.

The purpose of this paper is to develop simple semi-empirical transmission loss formulas that capture the main features of underwater sound propagation using the fewest possible environmental parameters. The purpose of the comparison is not to reproduce the site-specific details of the transmission losses, but for fast engineering-type assessments in applications that do not require high-

fidelity analysis and fine details of the sound field. Our approach will be based on simplified processes of the propagation physics and empirical measurements. In this development, we extended and combined work by previous authors to better account for the effects of the seafloor on waterborne sound propagation.

The formulas are useful for estimating sound transmission losses in generic yet representative underwater environments where detailed environmental knowledge is lacking or the fine details of underwater sound propagation is not required. Their use may offer advantages in situations such as the following:

- Sonar design, concept development, performance predictions, and analysis of the effectiveness of sonar operations in generic representative environments; e.g., the frequency regions where acoustic sensing is more effective;
- Broad analysis of the effects of radiated noise reduction on the platform's acoustic stealth, e.g., the frequency regions where noise reduction is more effective to avoid detection;
- Applications that require real-time rapid transmission loss calculations on low-powered processing platforms, such as on-board processing and mission planning by unmanned underwater systems;
- Real-time acoustic simulation as part of training systems to enhance sonar detection or to improve acoustic stealth via exploitation of the shallow water environment.

The analytical formulas have only a few input parameters and can be easily embedded into a spreadsheet program or other analytical expressions for further applications. Other situations for the use of these simple (and robust as will be shown by the examples) formulas is that often uncertainties and lack of knowledge about the underwater environment and their spatial and temporal variabilities means that the use of complex mathematical/numerical models do not necessarily produce outputs that are closer to reality in these situations.

2. Sound Transmission in Shallow Water Duct

In this paper, we are concerned about long range underwater sound propagation in shallow water where the range is many times of the water depth. In these situations, energy propagating at small grazing angles dominates because energy propagating at steeper angles quickly leaks into the seafloor. So we are mainly interested in the reflective properties of the seafloor and sea surface at small grazing angles. The transmission loss formulas we consider in this paper pertain to sound intensities that have been incoherently averaged over a suitable window of range, frequency, or depth. The aim is to capture the main features rather than the fine structures of underwater sound propagation.

2.1 Bottom reflection loss

At small grazing angles, the reflection loss from the seafloor, defined (in Neper) by the bottom reflection coefficient V_B as $-\log_e|V_B|$, is often proportional to grazing angle θ , and the magnitude of the bottom reflection coefficient can be approximated as,

$$|V_B| = \begin{cases} \exp(-Q_B\theta), & 0 \leq \theta \leq \theta^* \\ 0, & \theta > \theta^* \end{cases} \quad (1)$$

where θ^* is an angle of choice that separates a low loss region at small grazing angles where the loss in Neper $-\log_e|V_B| = Q_B\theta$ is proportional to grazing angle, from a high loss region where the loss is assumed to be infinite and therefore energy propagating beyond θ^* is ignored. Note that the reflection loss in dB is related to the loss gradient Q_B by the relation $-20\log_{10}|V_B| = [20\log_{10}(e)]Q_B\theta \approx 8.686Q_B\theta$.

Most unconsolidated sediments in shallow water have a compressional wave speed that is greater than the sound speed of the water just above the seafloor, and when the sediment is reasonably thick

(e.g., over a wavelength), a suitable choice for θ^* is the critical angle of reflection $\theta_c = \arccos(c_w/c_B)$, where c_w/c_B is the ratio of sound speeds at the water/bottom interface.

2.2 Harrison's expression

For shallow water environments where the sound speed profile is approximately constant and the seafloor reflectivity is approximated by Eq. (1), the distribution of propagating energy with grazing angle is approximately Gaussian, truncated by the angle θ^* . Integration of such an energy distribution, with careful treatment of energies whose grazing angles are less than that of mode 1, leads to the following expressions for the sound intensity I [Transmission Loss TL = $-10\log_{10}(I)$] [Harrison (2003), Table V]:

$$I = I_S [\text{erf}(W^*) - \text{erf}(W_2)] + I_1, \quad (2)$$

where

$$I_S = [\pi/(QH)]^{1/2} r^{-3/2}, \quad (3)$$

$$I_1 = \lambda/(rH^2) \exp(-W_1^2) \quad (4)$$

$$W^* = [Qr/H]^{1/2} \theta^*, \quad (5)$$

$$W_2 = [Qr/H]^{1/2} \theta_2, \quad \theta_2 = \min(1.5\theta_1, \theta^*) \quad (6)$$

$$W_1 = [Qr/H]^{1/2} \theta_1, \quad \theta_1 = \lambda_w/(2H), \quad \lambda_w = c_w/f, \quad (7)$$

where erf is the error function, H is water depth, r is horizontal range, f is sound frequency, c_w is sound speed in water. Note that we specified sea floor reflectivity using the magnitude of the reflection coefficient whereas Harrison used intensity reflection coefficient, and we have replaced Harrison's loss gradient parameter α by our parameter Q using the relation $\alpha = 2Q$. Later we will extend the parameter Q to include the effects of sea surface reflection loss.

In the first term of Eq. (2), I_S represents the effects of energy spreading and stripping by the boundary losses, leading to the so called "three-halves 3/2" spreading [$15\log(r)$] that lies between spherical [$20\log(r)$] and cylindrical spreading [$10\log(r)$]. Multiplication by the error function term captures the angular energy from mode 2 and up to the angle θ^* . The second term I_1 represents the contribution of mode 1, whose phase speed is associated with grazing angle θ_1 .

Whilst only the reflectivity, i.e., the magnitude of the reflection coefficient is explicitly considered in Harrison (2003,2005), the implicit assumption in the derivation of the formula is that the phase shifts associated with reflections from the seafloor are $-\pi$ at all grazing angles. Sea surface losses and sea water absorption were not considered in Harrison (2003).

3. Extension of Harrison's Formula

There are a few acoustic effects that were not accounted for in Harrison's formula. We extend Harrison's formula to account for the following effects:

- I. reflection phase shifts associated with evanescent wave excitation and mode penetration into the seafloor,
- II. seawater absorption,
- III. sea surface reflection losses.

Effect I is often important at low frequencies. Effect II is important at high frequencies. Effect III is important at high frequencies for high sea states or wind speeds. The extension to account for effects II+III is straightforward. The extension to account for effect I can be made straightforward by using the concept of “effective seafloor depth”. Harrison (2003) considered examples with bottom losses that are independent of frequency. We apply the extended Harrison formula to environments where bottom losses vary with frequency.

3.1 Effective depth approximation

3.1.1 Bottom reflection phase shift

For the most common case where the sound speed ratio c_w/c_B at the water/bottom interface is less than one, the sound wave also undergoes a phase shift when it is reflected from the seafloor at small grazing angles, due to the excitation of evanescent waves in the seafloor. The phase shift, when being referenced to that of a pressure-release surface ($-\pi$), often varies linearly with $\sin\theta$ at small grazing angles (note that $\sin\theta \approx \theta$ for small θ) (Chapman, 2001). Hence we may rewrite Eq. (1) to include the phase of the complex reflection coefficient,

$$V_B = \begin{cases} \exp(-Q_B\theta)\exp[i(-\pi + P\sin\theta)], & 0 \leq \theta \leq \theta^* \\ 0, & \theta > \theta^* \end{cases} \quad (8)$$

where P is the phase gradient with grazing angle.

In underwater acoustics modelling or geo-acoustic inversion, the effect of the seafloor is often modelled using fluid or solid layer structures, each layer is specified by three (for fluid layers, density, compressional wave speed and attenuation) or five parameters (for solid layers, additional shear wave speed and attenuation). With this approach, a larger number of unknown parameters need to be estimated. Moreover, the estimated geo-acoustic parameters and structures are not unique because a large family of such parameters can give the same acoustically equivalent effect to the waterborne sound (Chapman, 2001). In the simplified description in Eq. (8), the effect of the seafloor is specified by the complex reflection coefficient using three parameters, Q_B , θ^* , and P . For long range propagation involving small grazing angles, Eq. (8) provides a simple and effective parameterization of the seafloor effects. We will show later that for unconsolidated sediments, the phase gradient P can be approximated by $P = \pi/\sin\theta^*$ and the three parameters can be reduced to two.

We note in passing that under the approximation $\sin\theta \approx \theta$, the loss gradient Q_B and the phase gradient P in Eq. (8) can also be combined into a complex-valued reflection phase gradient for the acoustic characterization of seafloor effects (Joseph, 2003).

3.1.2 Effective depth and mode penetration

For the waterborne sound, the phase shift upon reflection from the water/seafloor boundary can be emulated by introducing an imaginary pressure release boundary shifted ΔH below the physical seabed, leading to the concept of effective depth (Chapman et al. 1989, Zhang and Tindle, 1993). For the phase shifts specified in Eq. (8), the effective depth is

$$\Delta H = P\lambda_w/(4\pi) \quad (9)$$

where λ_w is the acoustic wavelength in water. When the effective depth concept is applied to normal mode formulation of acoustic propagation, the effective depth is a measure of the penetration depth of the modes into the seafloor (Buckingham, 1979). The mode propagation angles in Harrison (2003) were calculated based on the seafloor being a pressure release surface without the effective depth, i.e., mode penetration into the seafloor was ignored. This approximation can be accurate at high frequencies when mode penetration into the seafloor is small. At lower frequencies, penetration into

the seafloor is greater and the effect can become significant. An easy way to account for this effect is to use the following effective water depth, H_e to replace the real water depth H in Eqs. (2) to (7):

$$H_e = H + \Delta H \quad (10)$$

For seafloors modelled as homogeneous, viscoelastic solids, the phase gradient P is given by (Chapman et al., 1989):

$$P = \varepsilon \pi / \sin \theta_c, \quad \varepsilon = (1 - 2c_s^2 / c_w^2)^2 (2\rho_b / \rho_w) / \pi \quad (11)$$

where c_w, ρ_w is the water sound speed and density, c_s, ρ_b are the shear wave speed and density in the bottom seafloor, respectively. Based on the data compiled in Hamilton (1980), we found that for most unconsolidated sediments ranging from coarse sand to clay-silt, the density and shear wave speeds are such that the parameter ε is close to unity. In all the examples of this paper, we used $\varepsilon = 1$. That is, the effective water depth is given by

$$H_e = H + \lambda_w / (4 \sin \theta_c) \quad (12)$$

which for a typical critical angle of about 20 degrees corresponds to a phase gradient of $P = 9.2$, which is consistent with the inversion results of P values of 11.5 for 100-200 Hz at a sandy-silt site in the East China Sea (Ge et al., 2004).

We can see from Eq. (7) that the introduction of the effective depth has the effect of lowering mode eigenvalues and propagation angles. Eq. (12) shows the addition to water depth is in the order of a wavelength, which becomes significant at low frequencies when the wavelengths approach a fraction of the water depth.

3.2 Frequency dependence of bottom loss gradient

Bottom losses from seafloors can be from a number of loss mechanisms, whose contribution may vary differently with frequency. In particular, recent studies on many shallow water sites around the world indicates the effective sediment attenuation in sandy-silt bottoms varies nonlinearly with frequency (Zhou, 2009, 2012), leading to frequency-dependent bottom loss. The variation of physical properties with depth is a factor for the frequency dependence. Some other factors and their frequency dependence are discussed below.

3.2.1 Excitation of propagating and evanescent waves

If the seafloor is approximated as homogeneous viscoelastic layers, the following mechanisms may contribute to the energy loss associated with reflections at small grazing angles,

- A. generation of propagating compressional waves in the bottom (that carries energy downwards),
- B. absorption of propagating compressional waves in the bottom,
- C. absorption of evanescent compressional waves in the bottom,
- D. generation of propagating shear waves in the bottom (that carries energy downwards),
- E. absorption of propagating shear waves in the bottom,
- F. absorption of evanescent shear waves in the bottom.

The importance of each mechanism depends on the type of seafloor and the sound frequency. For unconsolidated sediments whose compressional wave speed is higher than that of bottom water (e.g., fine sand), loss mechanisms C+D+E applies and mechanism C tends to dominates. For soft sedimentary rock (e.g., chalk or calcarenite), the same mechanisms C+D+E exists and mechanism D dominates. For hard rock (e.g., basalt, granite) seafloor, mechanisms C+F applies and mechanism F

tends to dominate. For very fine sediments (clay) whose sound speed is slightly less than that of bottom water, mechanism A+B applies and mechanism A dominates.

Generally the contribution of the propagation mechanisms (e.g., D) to bottom loss is essentially independent of frequency. For sandy-silt sediments, the contribution of the absorption mechanism C to bottom loss varies with frequency with an exponent between 0.5 and 1.0 at low frequencies (< 2000 Hz), and approaches almost frequency-independent at high frequencies (above 10 kHz) (Zhou et al., 2009,2012). (Note that if sediment absorption varies with frequency as $\propto f^n$, then its contribution to bottom loss will vary with frequency as $\propto f^{n-1}$. This is because bottom loss is proportional to the penetration depth of the evanescent waves into the seabed, which is inversely proportional to frequency $\propto f^{-1}$).

3.2.2 Interface and volume scattering

Real seafloors are not homogeneous and contain random volume inhomogeneities within the sediments and randomly rough interfaces between the sediment layers. Scattering from these inhomogeneities also contribute to the energy loss associated with bottom reflections.

The importance of the scattering mechanisms on bottom loss depends on the seafloor and the sound frequency. Whilst there has been much research on the contribution of interface and volume scattering on bottom scattering strength for modelling reverberation, research on the contribution of interface and volume scattering to bottom loss is limited and not mature enough in a form to be readily included in bottom loss calculations. For example, while acknowledging that scattering may increase bottom loss substantially, the geoacoustic bottom interaction model (GABIM) developed by University of Washington does not account for the effect of scattering on bottom loss (Jackson et al., 2010).

Rigorously speaking, the propagation and scattering mechanisms are coupled and need to be considered as a whole. In practice, scattering is often separately treated under the small perturbation approximation, and the effect of scattering superimposed on that of propagation.

For rough interface scattering, the scattering loss to the specularly reflected (coherent) component results from energy being scattered away from the specular direction. Under the condition of small grazing angles and large correlation lengths, perturbation approximation yields that the scattering loss obeys the form of our Eq. (1), i.e., proportional to the grazing angle, with the loss gradient Q being proportional to the 3/2 power of frequency (Eq. (9.6.6) Brekhovskikh and Lysanov 2003, Zhang 2013).

Scattering intensity from isotropic volume inhomogeneities whose size is much smaller than a wavelength vary with the 4th power of frequency (Rayleigh scattering) (Eq. (10.2.24), Brekhovskikh and Lysanov 2003). This means that the contribution to bottom loss gradient Q from scattering of evanescent waves by small-size sediment inhomogeneities will vary with the 3rd power of frequency. Later we will use this understanding to explain and model the rapid decay of acoustic propagation at high frequencies in the Barents Sea. Generally, in terms of the contribution to bottom losses, the mechanisms in the previous section dominate at low frequencies and scattering losses are more important at high frequencies.

3.2.3 Effective properties of sandy-silt bottoms

Low frequency long range acoustic measurements using various independent inversion techniques show that sandy-silt bottoms at many shallow water locations around the world have consistent geoacoustic properties (Zhou et al., 2009):

- The sediment/water sound speed ratio is about 1.06, which corresponds to a critical angle of 20 degrees;
- The effective compressional wave attenuation, α_B , vary nonlinearly with frequency $\alpha_B \propto f^n$, with the frequency exponent n lies between 1.5 and 2.0, with a mean of 1.8. This leads to an effective parametrisation for the bottom loss gradient Q :

$$Q_B(f) = Q_B(f = 1 \text{ kHz})(f / 1000)^{n-1} \quad (\text{Neper/m}) \quad (13)$$

where $Q_B(f = 1 \text{ kHz})$ may range from 0.5 to 2 with a mean around 1.3 Neper/rad. The frequency exponent is reduced by 1 because the evanescent sound penetration into the seafloor is inversely proportional to frequency.

Real sediments are not completely homogeneous and contain various vertical and horizontal inhomogeneities. However, simpler seafloor models may be used to produce equivalent acoustic effects for long range, waterborne sound propagation. The resulting seafloor model should be treated as the seafloor's effective acoustic equivalents with parameters that are "acoustically" averaged values over the propagation paths. The effective seabed attenuation obtained via geoacoustic inversion of a simple fluid bottom may include the contribution of the loss mechanisms C+D+E discussed in section 3.2.1 and the scattering loss mechanisms discussed in section 3.2.2. In particular, it has been shown that shear-wave supporting seafloors are acoustically equivalent to fluid seafloors of reduced density and increased attenuation (Zhang and Tindle, 1995) if the shear wave speed is less than about 500 m/s.

3.3 Sea surface loss

There are also losses associated with reflections from the sea surface due to scattering from the rough sea-air interface and scattering, absorption, and refraction effects of wind-generated bubbles underneath. Much work has been done on sea surface reflection loss (Eller, 1985) due to roughness (Chapman 1983; Zhang 2013) and bubbles (Ainslie 2005, Jones et al. 2012). Under the small angle approximation, the surface loss is proportional to grazing angle and we approximate the surface reflection coefficient V_S as,

$$V_S = \exp(-Q_S \theta) \exp(-i\pi), \quad 0 \leq \theta \leq \pi/2 \quad (14)$$

where Q_S is the loss gradient and the phase shift is that of a pressure release surface ($-\pi$). Sea surface losses can be readily included by using a loss gradient Q that combines the bottom and surface reflection coefficients, that is:

$$|V_B V_S| = \exp(-Q\theta), \quad Q = Q_B + Q_S, \quad 0 \leq \theta \leq \theta^* \quad (15)$$

A simple semi-empirical formula, based on the measurements of Weston and Ching (1989) is adopted here:

$$Q_S = 3.8(f/1000)^{3/2}(U/10)^4, \quad \text{Neper/rad} \quad (16)$$

where U is the wind speed in m/s measured at 10 m height above water level.

3.4 Seawater absorption

The effect of seawater absorption is included by multiplying the intensities by the factor:

$$L_A = \exp(-2\alpha_A r) \quad (17)$$

where the parameter α_A is absorption coefficient in Neper/m, which is due to chemical relaxations and viscosity and its magnitude depends on frequency, sea water temperature, salinity, pressure (depth), and acidity (pH value). In this paper, we use the Francois-Garrison equation when water temperature, salinity, pressure, and acidity are known (or can be estimated) and the Thorp equation as in Urick (1983) for standard water conditions when these parameters are unknown.

4. Model-Data Comparison

Next we use the simple analytical expressions to compare with transmission loss measurements at several sites worldwide. Each site has specific environment properties (e.g., water mass sound speed profiles and sea bottom properties). Because of the deliberately simple nature of our expressions, the purpose of the comparison is not to reproduce the site-specific details of the transmission losses, but to show that the simple expressions are capable of reproducing the general propagation characteristics, which makes them useful for fast, site-generic studies.

All our examples used Eqs. (2) to (7) with the water depth H replaced by the effective depth H_e given by Eq. (12). The only other inputs we used to calculate the transmission losses versus range-frequency plots below are the loss gradient Q and critical angle θ_c .

4.1 English Channel

Figure 1 compares transmission loss data collected from a site in the English Channel with calculations from the formulas. The only environmental information we have about the site is the water depth of 90 m. In addition, we used the following inputs for our calculations.

- the critical angle is 20 degrees, the mean value from 9 shallow water, sandy-silt locations around the world (Zhou, 2009, Fig. 8);
- The loss gradient Q varies with frequency as:

$$Q = 1.3(f/1000)^{0.4} \quad (18)$$

where the Q value at 1 kHz, 1.3, was an average of the data for 21 shallow water, sandy-silt locations around the world (Zhou, 2009, Fig. 7). The frequency exponent 0.4 was obtained by trial and error (“inversion” by visual inspection) to match the optimum frequencies of propagation between 200 – 400 Hz. This value is in the lower bound of the frequency dependence shown by the same data. The lower value could be due to the excitation of propagating shear waves, which induces a frequency-independent bottom loss and hence decreases the frequency dependence.

We see that adding seawater absorption is necessary to match the data at high frequencies. At low frequencies, because of the neglect of mode penetration into the seafloor, Harrison’s expression yields a rapid increase in transmission losses as the frequencies decrease from about 50 Hz. This low-frequency roll-off is much sharper than that shown in the data. Using the “effective depth” to account for mode penetration into the seafloor yields a less abrupt roll-off with decreasing frequencies, which significantly improves the agreements with data, as shown by the bottom right plot in Figure 1.

Note that the low-frequency roll-off is not the usual waveguide cut-off phenomena. The low-frequency roll-off is due to the propagation angle of mode 1 steepening with decreasing frequency. The steepening angle leads to increasing attenuation because of greater bottom losses per bounce and more bottom bounces per unit range. The low-frequency roll-off occur when the angle of mode 1 moves away from zero grazing angle whereas the low-frequency cut-off occur when the same angle approaches the critical angle. Generally there are still several modes propagating when low frequency roll-off occurs. In our case above, the waveguide cutoff frequency is 13 Hz, and the roll-off started several times of the cut-off frequency.

Using basically mean properties of sandy-silt sediments from other sites of the world, we are able to produce a reasonable match to the main features of the data by simply adjusting one parameter – the exponent of the frequency dependence of Q . There were some detailed features of the sound field that we were unable to produce, probably due to our neglect of the depth variation of the sound speed profile and the source and receiver positions. The presence of the optimum frequencies around 200 Hz are the competing results of greater losses due to steepening of the modal angles at low frequencies and the greater losses due to sea water absorption at high frequencies. The locations of the optimum frequencies are particularly sensitive to the frequency exponent of the Q parameter.

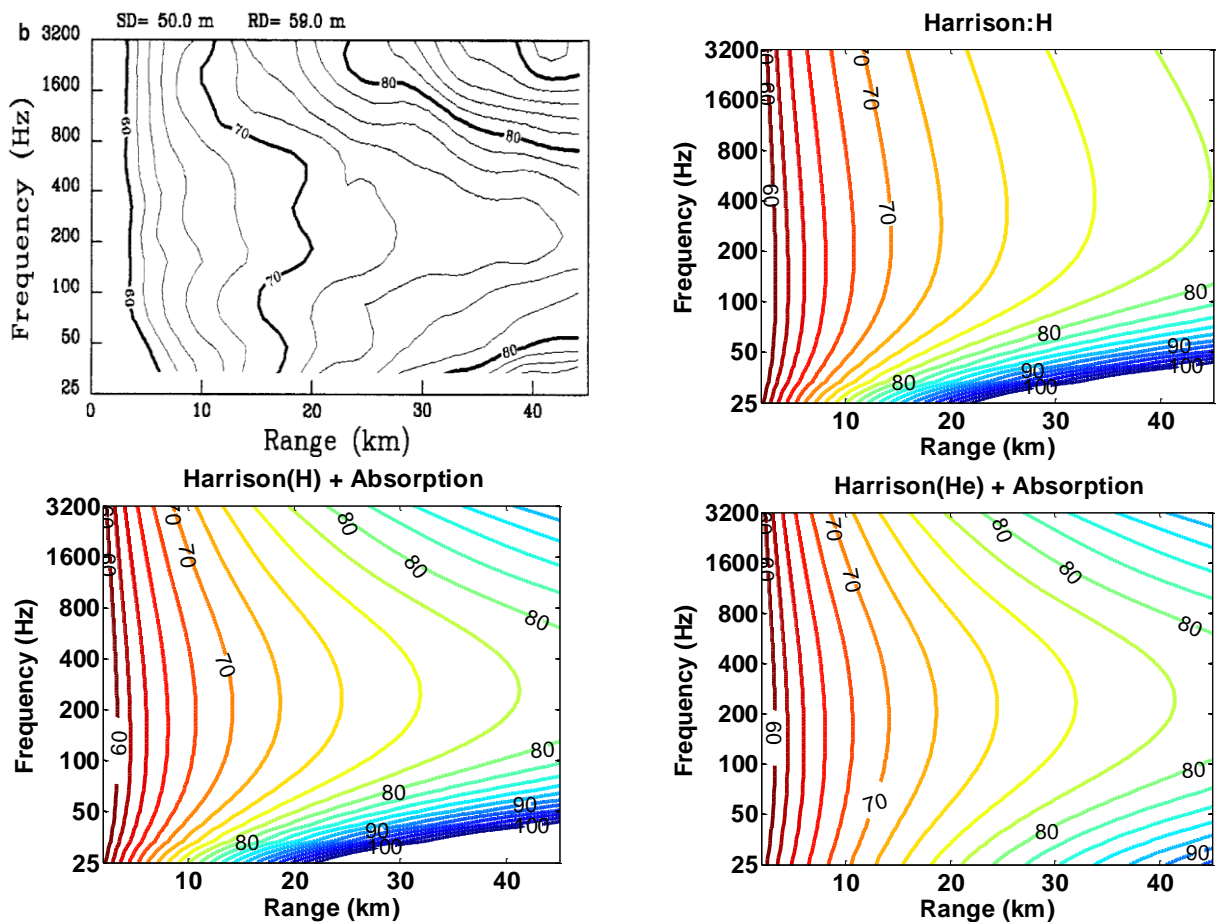


Figure 1. Transmission losses versus frequency and range in English Channel: comparison of measurements and outputs from formulas. (top left) measurements from Jensen et al. (2011); (top right) Harrison's formula; (bottom left) Harrison's formula plus absorption; (bottom right): Harrison's formula using effective depth plus absorption.

4.2 East China Sea

We now compare our model predictions with data collected at two shallow water sites in the East China Sea. The two sites are of similar depth (circa 100 m) and separated by about 200 km. The data were collected at different seasons with different, downward-refracting sound speed profiles.

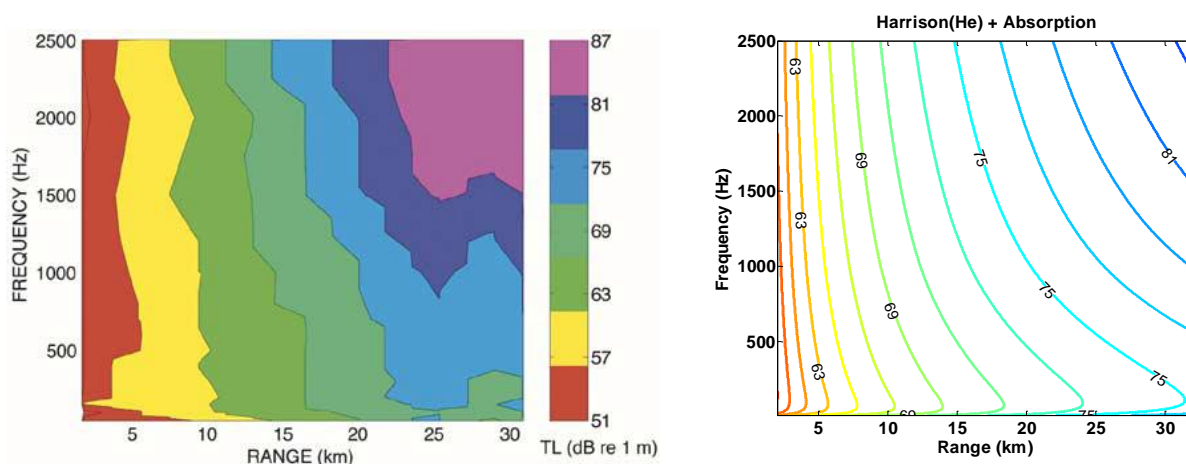


Figure 2. Transmission losses versus frequency and range at the ASIAEX site in the East China Sea: comparison of measurements and outputs from formulas. (left) data (Dahl et al. (2004), Fig. 7) (right) The modified Harrison's formula plus absorption.

The first set of transmission loss (TL) and related environmental data was collected in June 2001 during the Asian Seas International Acoustics Experiment (ASIAEX) with participants from the United States, China, Taiwan, and Korea (Dahl et al. 2004). The second set of transmission loss data was measured in September by the Naval Air Warfare Center (USA) under the Harsh Environmental Program (HEP) (Abbot et al. 2003). The sediments in the area at both sites are fine sand and silty sand of variable thickness, layering, and grain size compositions over harder subbottom sediments layers. Complex geoacoustic modelling and propagation models have been used to infer the sediment properties to match the TL data (Peng et al. 2004; Abbot et al. 2003, 2006). Both sets of data show similar propagation characteristics and we use the same seafloor input parameters based on the environmental information in Peng et al. (2004):

- a critical angle 20 degrees, the mean value from 9 shallow water, sandy-silt locations around the world (Zhou, 2009, Fig. 8);
- the loss gradient Q vary with frequency as (Peng et al. 2004):

$$Q = 0.51(f/1000)^{0.55} \tag{19}$$

- Sea surface loss is for a wind speed of 3 m/s.

Sea water absorption was calculated based on the CTD measurements in Peng et al. (2004) and acidity information in Ainslie (2010). We make the following observations:

- Although we ignored the downward-refracting effects of the sound speed profiles and also used simple representations of the complex seafloor structures (Peng et al. 2004; Abbot, 2003), our formulas were able to give reasonable matches to the measurements, as shown by Figures 2 and 3. The effects of the sound speed profile need further investigation, but we note that the transmission losses in the first set of data were depth-averaged across receives in the water.
- The optimum frequency is around 100 Hz, less than half of that shown by the data of the English Channel. The increase in water depth (from 90 to 104 m) contributed slightly. But the main contribution is the increase of the frequency exponent of the Q parameter from 0.4 for the English Channel to 0.55 for the East China Sea site. With a greater exponent, as frequency decreases from the value at 1 kHz, the bottom loss decreases faster with decreasing frequency, favouring lower frequency propagation.

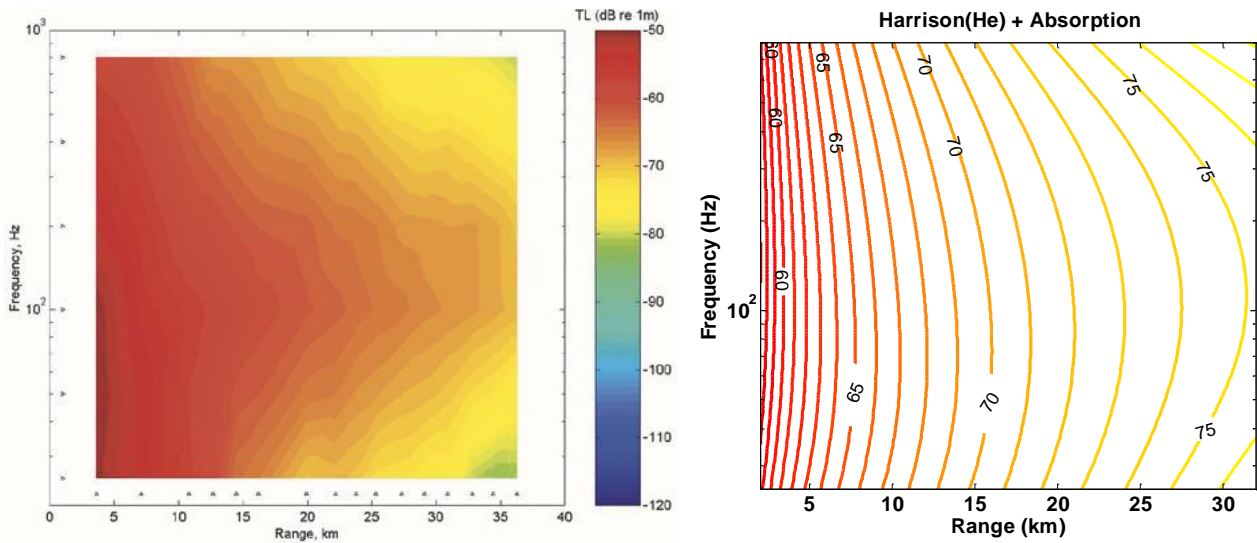


Figure 3. Transmission losses versus frequency and range at the HEP site in the East China Sea: comparison of measurements and outputs from formulas. (left) Figure 8a from Abbot et al. (2003); (right) The modified Harrison's formula plus absorption.

4.3 Barents Sea

Figure 4 compares transmission loss data collected from a site of 60 m in the Barents Sea with our calculations. The measurement data can be directly compared with those in Fig. 1 for the English Channel. We notice the much higher transmission losses overall, and in particular, the rapid fall off of energy below 200 Hz, and the higher decay rate with range above 2000 Hz. Core analysis indicates the upper 60 cm of the sediment consists of gravel intermixed with sand with postulated compressional wave speed of 1800 m/s and density of 2.0 g/cm³. To match the high losses at frequencies below 400 Hz, Jensen (1991) developed two plausible geoacoustic models, either a thick layer of glacial till with a shear speed of around 700 m/s or a thin (0.5–3 m) layer of glacimarine sediments over a sandstone/shale substrate. In both cases, the high losses at low frequencies were attributed to coupling of the waterborne energy into shear waves in the seabed.

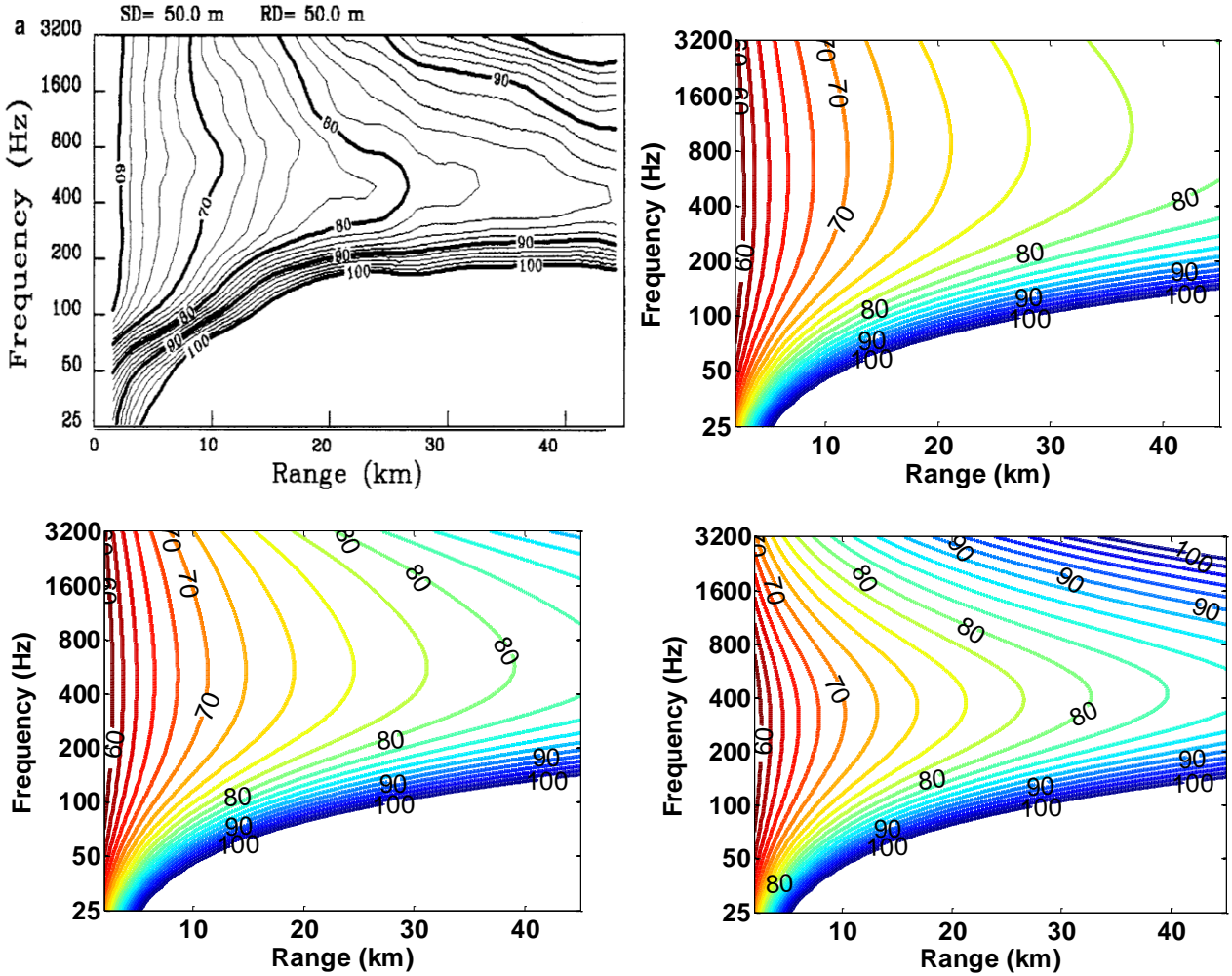


Figure 4. Transmission losses versus frequency and range in the Barents Sea in 60 m water depth exhibiting extreme losses at frequencies below 200 Hz. Top left: Measurements data from Jensen (1991). Top right: Formula prediction without seawater absorption, without sediment volume scattering. Bottom left: Formula with seawater absorption but without sediment volume scattering. Bottom right: Formula with seawater absorption and with sediment volume scattering.

We adopt Jensen's homogeneous elastic geoacoustic model, and use a critical angle of 36 degrees, which corresponds to the water/sediment sound speed ratio in Table I of Jensen (1991). Our loss gradient Q has three components,

$$Q = 1.3 + 1.0(f/1000) + Q_{Bs}, \quad Q_{Bs} = 8.0(f/1000)^3 \quad (20)$$

The first term, 1.3 Neper/radian, represents the contribution of the loss mechanisms of propagating shear waves (mechanism D discussed in section 3.1), which is independent of frequency and is calculated for a shear wave speed of 650 m/s (Eq. (10), Zhang and Tindle, 1995). The second term represents the loss mechanism of evanescent wave absorption, which is proportional to frequency and is taken from Zhou and Zhang (2012, Fig.4) for typical sandy-silt sediments. The third term represents the loss mechanism of sediment volume scattering, which is proportional to the third power of frequency and being added to match the rapid decay rate shown by the data above 2000 Hz. As shown by the plots in Fig.4, we found that seawater absorption is insufficient to produce the rapid decay rate above 2000 Hz.

Katsnelson and Petnikov (2012) noted that one characteristic of the sediments in the Barents Sea is the existence of abrupt random inhomogeneities and most regions of the Barents Sea can be considered as randomly inhomogeneous medium. As noted by Jensen (1991), the core analysis of the site shows gravel and sand mixtures. Therefore it is plausible that the decay rate in excess of those sea water absorption is due to sediment volume scattering. The gravel particles are much smaller than the wavelengths at the frequencies concerned, Rayleigh scattering dominates and scattering-induced sediment attenuation should be proportional to the 4th power of frequency. Because the penetration of the compressional evanescent wave into the sediment is inversely proportional to frequency, the scattering-induced bottom loss should be proportional to the 3rd power of frequency. Hence we postulated that the scattering-induced loss gradient is proportional to the 3rd power of frequency. The value at 1 kHz, 8.0, is chosen to match the rapid decay of data above 2000 Hz.

The bottom loss at low frequencies is nearly frequency-independent, which yields the rapid roll-off below 200 Hz. This rapid roll-off is similar in nature to those shown for propagation over calcarenite seafloor off Western Australia coast (Duncan et al. 2009). The bottom loss plus seawater absorption at high frequencies is strongly frequency-dependent, which yields the rapid decay above 2000 Hz. The competition of these losses mechanisms produces the optimum frequencies around 400 Hz.

5. Concluding Remarks

We extended work of previous authors to better account for the effects of the seafloor on waterborne sound propagation and gave a simple formula for shallow water sound transmission by taking into account the effects of energy spreading, absorption, and leakage out of boundaries. Comparison with measurement data shows that the formula are capable of reproducing the main features of shallow water sound propagation at several shallow water sites around the world with seafloors of different acoustic reflective properties. The formula is useful for estimating sound transmission losses for quick analysis of sonar operations or acoustic stealth in generic yet representative underwater environments where detailed environmental knowledge is lacking or the fine details of underwater sound propagation is not required. The formula has only a few input parameters and can be easily embedded into a spreadsheet program or other analytical expressions for further applications.

Besides the data-comparison examples given in this paper, we have also tested the formula against data collected in other environments with seafloors of unconsolidated sediments, including two sites in the Southern East China Sea (Emerson et al. 2015) and a site in the Mediterranean Sea (Murphy and Olesen, 1976), where similarly good fits were achieved. The formula is not very sensitive to the particular value of angle θ^* as long as it is greater than about 15 degrees. For seafloors of unconsolidated sediments, the angle θ^* can be set to a default value of 20 degrees (that of the “effective sandy-silt bottom” discussed in section 3.2) if the critical angle of reflection is unknown. The formula can also be applied to other types of seafloors, e.g., sedimentary rock, by suitable choice of the effective parameters in Eq. (8). The result of this application will be reported in a future publication. Future extensions also include consideration of sound speed variations with depth.

Acknowledgements

I thank Chris Gillard for critical reading and discussions, which helped improve the paper.

References

- [1] Abbot, P., Celuzza, S., Dyer, I., Gomes, B., Fulford, J. and Lynch, J. "Effects of East China Sea shallow-water environment on acoustic propagation", *IEEE Journal of Oceanic Engineering*, **28**(2), 192-211 (2003).
- [2] Abbot, P., Dyer, I. and Emerson, C. "Acoustic propagation uncertainty in the shallow East China Sea", *IEEE Journal of Oceanic Engineering*, **31**(2), 368-383 (2006).
- [3] Ainslie, M.A. *Principles of Sonar Performance Modeling*, Springer-Praxis, 2010.
- [4] Ainslie, M. "Effect of wind-generated bubbles on fixed range acoustic attenuation in shallow water at 1 – 4 kHz", *Journal of the Acoustical Society of America*, **118**, 3513-3523 (2005).
- [5] Brekhovskikh, L.M. and Lysanov, Y.P. *Fundamentals of Ocean Acoustics*, 3rd ed. Springer-Verlag, Berlin, 2003.
- [6] Buckingham, M. "Array gain of a broadside vertical line array in shallow water", *Journal of the Acoustical Society of America*, **65**(1), 148-161 (1979).
- [7] Chapman, D.M.F. "An improved Kirchhoff formula for reflection loss at a rough ocean surface at low grazing angles", *Journal of the Acoustical Society of America*, **73**, 520-527 (1983).
- [8] Chapman, D.M.F., Ward, P.D. and Ellis, D.D. "The effective depth of a Pekeris ocean waveguide, including shear wave effects", *Journal of the Acoustical Society of America*, **85**, 648-653 (1989).
- [9] Chapman, D.M.F. "What are we inverting for?" in *Inverse Problems in Underwater Acoustics*, edited by M. I. Taroudakis and G. Makrakis, Springer, Berlin, pp. 1–14. 2001.
- [10] Duncan, A., Gavrilov, A, and Fan, L. "Acoustic propagation over limestone seabeds", *Proceedings of Acoustics 2009: Research to Consulting*, Adelaide, Australia, 23-25 November 2009, pp. 291-296.
- [11] Eller, A.I. and Gershfeld, D.A. "Low frequency acoustic response of shallow water ducts", *Journal of the Acoustical Society of America*, **78**, 622-631 (1985).
- [12] Eller, A. "Implementation of rough surface loss in sonar performance models", *Oceans*, **17**, 494-498 (1985).
- [13] Emerson, C., Lynch, J.F., Abbot, P., Lin, Y., Duda, T.F., Gawarkiewicz, G.G. and Chen, C. "Acoustic propagation uncertainty and probabilistic prediction of sonar system performance in the Southern East China sea continental shelf and shelfbreak environments", *IEEE Journal of Oceanic Engineering*, **40**(4), 1003-1017 (2015).
- [14] Etter, P.C. *Underwater Acoustic Modeling and Simulation*, CRC Press, Boca Raton, FL, 2013.
- [15] Ge, H., Zhao, H., Gong, X. and Shang, E. "Bottom-reflection phase-shift estimation from ASIAEX data", *IEEE Journal of Oceanic Engineering*, **29**(4), 1045-1049 (2004).
- [16] Hamilton, E.L. "Geoacoustic modeling of the sea floor", *Journal of the Acoustical Society of America*, **68**, 1313-1339 (1980).
- [17] Harrison, C.H. "Closed-form expressions for ocean reverberation and signal excess with mode stripping and Lambert's law", *Journal of the Acoustical Society of America*, **114**, 2744–2756 (2003).
- [18] Jackson, D., Odom, R., Boyd, M. and Ivakin, A. "A Geoacoustic Bottom Interaction Model (GABIM)", *IEEE Journal of Oceanic Engineering*, **35**(3), 603-617 (2010).
- [19] Jackson, D.R., Odom, R.I., Boyd, M.L. and Ivakin, A.N. "Corrections to "A Geoacoustic Bottom Interaction Model (GABIM)", *IEEE Journal of Oceanic Engineering*, **36**(2), 373 (2011).
- [20] Jensen, F., Kuperman, W., Porter, M. and Schmidt, H. *Computational Ocean Acoustics*, Springer-Verlag, 2011.
- [21] Jones, A.D., Duncan, A.J., Bartel, D.W. Zinoviev, A. and Maggi, A.J. "A physics-based model of surface reflection loss for ray models", *Proceedings 11th European Conference on Underwater Acoustics*, Edinburgh, 2-6 July 2012, pp. 77-84.
- [22] Joseph, P. "Complex reflection phase gradient as an inversion parameter for the prediction of shallow water propagation and the characterization of sea-bottoms", *Journal of the Acoustical Society of America*, **113**, 758-768 (2003).
- [23] Katsnelson, B., Petnikov, V. and Lynch, J. *Fundamentals of Shallow Water Acoustics*, Springer Science, 2012.
- [24] Murphy, E. and Olesen, O.V. "Intensity-range relations for shallow-water sound propagation", *Journal of the Acoustical Society of America*, **59**, 305–311 (1976).
- [25] Tindle, C.T. and Weston, D.E. "Connection of acoustic beam displacement, cycle distances, and attenuations for rays and normal modes", *Journal of the Acoustical Society of America*, **67**(5), p. 1614 (1980).
- [26] Urlick R.J. *Principles of Underwater Sound*, 3rd edition, Peninsula Publishing, 1983.
- [27] Weston, D.E. "Intensity-range relations in oceanographic acoustics", *Journal of Sound and Vibration*, **18**, 271–287 (1971).
- [28] Weston, D.E. and Ching, P.A. "Wind effects in shallow-water acoustic transmission", *Journal of the Acoustical Society of America*, **86**(4), 1530–1545 (1989).
- [29] Weston, D.E. "Wave shifts, beam shifts, and their role in modal and adiabatic propagation", *Journal of the Acoustical Society of America*, **96**(1), 406-416 (1994).
- [30] Zhang, Z.Y. and Tindle, C.T. "Complex effective depth of the ocean bottom", *Journal of the Acoustical Society of America*, **93**, 205-213 (1993).
- [31] Zhang Z.Y. and Tindle C.T. "Improved equivalent fluid approximation for a low shear speed ocean bottom", *Journal of the Acoustical Society of America*, **98**, 3391-3396 (1995).
- [32] Zhang, Z.Y. "Predictions of sonar performance for a shallow water test case with rough boundaries", *Proceedings 1st International Conference and Exhibition on Underwater Acoustics*, Corfu, Greece, 23-28 June 2013.
- [33] Zhou, J., Zhang, X. and Knobles, D.P. "Low-frequency geoacoustic model for the effective properties of sandy seabottoms", *Journal of the Acoustical Society of America*, **125**(5), 2847-2866 (2009).
- [34] Zhou, J. and Zhang, X. "Shear wave velocity and attenuation in the upper layer of ocean bottoms from long-range acoustic field measurements", *Journal of the Acoustical Society of America*, **132**(6), 3698-3705 (2012).